

Entropic lattice Boltzmann method for microflows

S. Ansumali, I. V. Karlin*, C. E. Frouzakis, K. B. Boulouchos

Aerothermochemistry and Combustion Systems Laboratory
Swiss Federal Institute of Technology
CH-8092 Zurich, Switzerland

November 6, 2018

Abstract

A new method for the computation of flows at the micrometer scale is presented. It is based on the recently introduced minimal entropic kinetic models. Both the thermal and isothermal families of minimal models are presented, and the simplest isothermal entropic lattice Bhatnagar-Gross-Krook (ELBGK) is studied in detail in order to quantify its relevance for microflow simulations. ELBGK is equipped with boundary conditions which are derived from molecular models (diffusive wall). A map of three-dimensional kinetic equations onto two-dimensional models is established which enables two-dimensional simulations of quasi-two-dimensional flows. The ELBGK model is studied extensively in the simulation of the two-dimensional Poiseuille channel flow. Results are compared to known analytical and numerical studies of this flow in the setting of the Bhatnagar-Gross-Krook model. The ELBGK is in quantitative agreement with analytical results in the domain of weak rarefaction (characterized by Knudsen number Kn , the ratio of mean free path to the hydrodynamic scale), up to $Kn \sim 0.01$, which is the domain of many practical microflows. Moreover, the results qualitatively agree throughout the entire Knudsen number range, demonstrating Knudsen's minimum for the mass flow rate at moderate values of Kn , as well as the logarithmic scaling at large Kn . The present results indicate that ELBM can complement or even replace computationally expensive microscopic simulation techniques such as kinetic Monte Carlo and/or molecular dynamics for low Mach and low Knudsen number hydrodynamics pertinent to microflows.

1 Introduction

Gas flows at the micrometer scale constitute a major portion of contemporary fluid dynamics of engineering interest. Because of its relevance to the engineering of micro electro-

*Corresponding author

mechanical systems (MEMS), the branch of computational fluid dynamics focused on micro scale phenomena is often called “microfluidics” [1, 2].

Microflows are characterized by the Knudsen number, Kn , which is defined as the ratio of the mean free path of molecules λ and the characteristic scale L of variation of hydrodynamic fields (density, momentum, and energy). For typical flows in microdevices, $Kn \sim \lambda/L$ varies from $Kn \ll 1$ (almost-continuum flows) to $Kn \sim 1$ (weakly rarefied flows). Another characteristic property of microflows is that they are highly subsonic, that is, the characteristic flow speed is much smaller than the speed of sound. This feature is characterized by the Mach number, $Ma \sim u/c_s$, where u is the characteristic flow speed, and c_s is the (isentropic) speed of sound. Thus, for microflows, $Ma \ll 1$. To be more specific, typical flow velocities are about 0.2 m/s, corresponding to $Ma \sim 10^{-4}$, while values of the Knudsen number range between $10^{-4} \leq Kn \leq 10^{-1}$. Finally, in the majority of applications, microflows are quasi-two-dimensional.

Theoretical studies of gas flows at finite Knudsen number have begun several decades ago in the realm of the Boltzmann kinetic equation. To that end, we mention pioneering contributions by Cercignani, Sone, and others [3, 4]. These studies focused on obtaining either exact solutions of the stationary Boltzmann kinetic equation, or other model kinetic equations in relatively simple geometries (most often, infinite or semi-infinite rectangular ducts), or asymptotic expansions of these solutions.

While analytical solutions are important for a qualitative understanding of microflows, and also for the validation of numerical schemes, they certainly do not cover all the needs of computational fluid dynamics of practical interest. At present, two CFD strategies for microflows are well established.

- *Equations of continuous fluid mechanics with slip boundary conditions.* The simplest semi-phenomenological observation about microflows is the break down of the no-slip boundary condition of fluid mechanics with increasing Knudsen number. Since microflows are highly subsonic, this leads to the simplest family of models, equations of incompressible or compressible fluid dynamics supplemented by slip velocity boundary conditions (a review can be found in [2]). This approach, although widely used at the early days of microfluidics, remains phenomenological. Moreover, it fails to predict phenomena such as non-trivial pressure and temperature profiles observed by more microscopic approaches.
- *Direct simulation of the Boltzmann kinetic equation.* On the other extreme, it is possible to resort to a fully microscopic picture of collisions, and to use a molecular dynamics approach or a simplified version thereof - the Direct Simulation Monte Carlo method of Bird (DSMC) [5]. DSMC is sometimes heralded as the method of choice for simulation of the Boltzmann equation, and it has indeed proven to be robust in supersonic, highly compressible flows with strong shock waves. However, the highly subsonic flows at small to moderate Knudsen number is not a “natural” domain for the DSMC simulations where it becomes computationally intensive [6].

Since semi-phenomenological computations are not reliable, and the fully microscopic

treatment is not feasible, the approach to CFD of microflows must rely on reduced models of the Boltzmann equation. Two classical routes of reducing the kinetic equations are well known, the Chapman-Enskog method and Grad's moment method (for a modern summary and extensions of these methods see, for example, [7]). The Chapman-Enskog method extends the hydrodynamic description (compressible Navier-Stokes equations) to finite Kn in the form of a Taylor series, leading to hydrodynamic equations of increasingly higher order in the spatial derivatives (Burnett's hydrodynamics). Grad's method extends the hydrodynamic equations to a closed set of equations including higher-order moments (fluxes) as independent variables. Both methods are well suited for theoretical studies of microflows. In particular, as was already noted by Grad [8], moment equations are especially well suited for low Mach number flows.

However, applications of Grad's moment equations or of Burnett's hydrodynamics (or of existing extensions and generalizations thereof) to CFD of microflows are limited at present because of several reasons. The most severe difficulty is in formulating the boundary conditions at the reduced level. Although some studies of boundary conditions for moment systems were initiated recently [9], this problem is far from solved. The crucial importance of the boundary condition for microflows is actually expected. Indeed, as the rarefaction is increasing with Kn, the contribution of the bulk collisions becomes less significant as compared to the collisions with the boundaries, and thus the realistic modelling of the boundary conditions becomes increasingly important.

In this paper we set up a novel approach to the CFD of microflows. It is based on the recently developed Entropic Lattice Boltzmann Method (ELBM)[10, 11, 12, 13, 14, 15, 16, 17, 18, 19]. The choice of the ELBM for microflows is motivated by two reasons:

- ELBM is an unconditionally stable simulation method for flows at low Mach numbers.
- In contrast to Grad's method, ELBM is much more compliant with the boundary conditions. Recently, an appropriate boundary condition for the ELBM was found upon a discretization of the diffusive wall boundary condition of the Boltzmann equation [15]. This boundary condition was also rediscovered in [20], where ELBM simulations were tested against molecular dynamic simulations with a good agreement.

It should be mentioned that the predecessor of ELBM, the lattice Boltzmann method (LBM) [21], was employed several times for microflow simulations [22, 23, 24, 25]. The motivation of most of these works was the velocity slip observed in the LBM simulations using the so-called bounce-back boundary condition [22, 23, 24, 25]. However, since the bounce-back boundary condition is completely artificial, the results are questionable [20].

The outline of the present paper is as follows: In section 2, for the sake of completeness, we present the general description of isothermal and thermal entropic lattice Boltzmann models. Then, we describe the ELBM setup for the simplest situation of isothermal flows, the entropic lattice Bhatnagar-Gross-Krook model (ELBGK). The case of isothermal models is important in itself since it allows to study nontrivial flow phenomena such as velocity slip at the wall, and the well-known Knudsen minimum of the mass flowrate in pressure-driven channel flows. Prediction of the Knudsen minimum is a classical benchmark problem

for the simulation of microflows. In section 3, we describe in detail the implementation of the diffusive boundary conditions for the ELBM for two-dimensional simulations. A separate section 4 is devoted to the question of how to simulate quasi-two-dimensional flows with two-dimensional models, and how to map the parameters of the model onto experimental data and more microscopic simulations. In section 5, we present simulation results for the quasi-two-dimensional Poiseuille flow, and discuss Knudsen's minimum, comparing results with known asymptotic and analytic solutions to the Boltzmann kinetic equation. Results are discussed in section 6, where we define the domain of validity of ELBM for microflows. We also suggest a straightforward application of ELBM results to accelerate more microscopic simulation approaches like the DSMC method.

2 Minimal kinetic models

We start with a generic discrete velocity kinetic model. Let $f_i(\mathbf{x}, t)$ be populations of the D -dimensional discrete velocities \mathbf{c}_i , $i = 1, \dots, n_d$, at position \mathbf{x} and time t . The hydrodynamic fields are the linear functions of the populations, namely

$$\sum_{i=1}^{n_d} \{1, \mathbf{c}_i, c_i^2\} f_i = \{\rho, \rho \mathbf{u}, \rho DT + \rho u^2\}, \quad (1)$$

where ρ is the mass density of the fluid, $\rho \mathbf{u}$ is the D -dimensional momentum density vector, and $e = \rho DT + \rho u^2$ is the energy density. In the case of isothermal simulations, the set of independent hydrodynamic fields contains only the mass and momentum densities. It is convenient to introduce n_d -dimensional population vectors \mathbf{f} , and the standard scalar product, $\langle \mathbf{f} | \mathbf{g} \rangle = \sum_{i=1}^{n_d} x_i y_i$. For example, for almost-incompressible hydrodynamics (leaving out the energy conservation), the locally conserved density and momentum density fields are written as

$$\langle \mathbf{1} | \mathbf{f} \rangle = \rho, \quad \langle \mathbf{c}_\alpha | \mathbf{f} \rangle = \rho u_\alpha. \quad (2)$$

Here $\mathbf{1} = \{1\}_{i=1}^{n_d}$, $\mathbf{c}_\alpha = \{c_{i\alpha}\}_{i=1}^{n_d}$, and $\alpha = 1, \dots, D$, where D is the spatial dimension.

The construction of the kinetic simulation scheme begins with finding a convex function of populations H (entropy function), which satisfies the following condition: If $\mathbf{f}^{\text{eq}}(\rho, \mathbf{u})$ (local equilibrium) minimizes H subject to the hydrodynamic constraints (equations (1) or (2)), then \mathbf{f}^{eq} also satisfies certain restrictions on the higher-order moments. For example, the equilibrium stress tensor must respect the Galilean invariance,

$$\sum_{i=1}^{n_d} c_{i\alpha} c_{i\beta} f_i^{\text{eq}}(\rho, \mathbf{u}) = \rho c_s^2 \delta_{\alpha\beta} + \rho u_\alpha u_\beta. \quad (3)$$

The corresponding entropy functions for the isothermal and the thermal models were found in [26, 15, 16], and are given below (see section 2.0.4 and Table 1). For the time being, assume that the convex function H is given.

The next step is to obtain the set of kinetic equations,

$$\partial_t f_i + c_{i\alpha} \partial_\alpha f_i = \Delta_i. \quad (4)$$

Let $\mathbf{m}_1, \dots, \mathbf{m}_{n_c}$ be the n_d -dimensional vectors of locally conserved fields, $M_i = \langle \mathbf{m}_i | \mathbf{f} \rangle$, $i = 1, \dots, n_c$, $n_c < n_d$. The n_d -dimensional vector function Δ (collision integral), must satisfy the conditions:

$$\langle \mathbf{m}_i | \Delta \rangle = 0, \quad i = 1, \dots, n_c \quad (\text{local conservation laws}),$$

$$\langle \nabla H | \Delta \rangle \leq 0 \quad (\text{entropy production inequality}),$$

where ∇H is the row-vector of partial derivatives $\partial H / \partial f_i$. Moreover, the local equilibrium vector \mathbf{f}^{eq} must be the only zero point of Δ , that is, $\Delta(\mathbf{f}^{\text{eq}}) = \mathbf{0}$, and, finally, \mathbf{f}^{eq} must be the only zero point of the local entropy production, $\sigma(\mathbf{f}^{\text{eq}}) = 0$. Collision integrals which satisfies all these requirements are called admissible. Let us discuss several possibilities of constructing admissible collision integrals.

2.0.1 BGK model

Suppose that the entropy function H is known. If, in addition, the local equilibrium is also known as an explicit function of the locally conserved variables (or some reliable approximation of this function is known), the simplest option is to use the Bhatnagar-Gross-Krook (BGK) model. In the case of isothermal hydrodynamics, for example, we write

$$\Delta = -\frac{1}{\tau} (\mathbf{f} - \mathbf{f}^{\text{eq}}(\rho(\mathbf{f}), \mathbf{u}(\mathbf{f}))). \quad (5)$$

The BGK collision operator is sufficient for many applications. However, it becomes advantageous only if the local equilibrium is known in a closed form. Unfortunately, often only the entropy function is known but not its minimizer. For these cases one should construct collision integrals based solely on the knowledge of the entropy function. We present here two particular realizations of the collision integral based on the knowledge of the entropy function only.

2.0.2 Quasi-chemical model

For a generic case of n_c locally conserved fields, let \mathbf{g}_s , $s = 1, \dots, n_d - n_c$, be a basis of the subspace orthogonal (in the standard scalar product) to the vectors of the conservation laws. For each vector \mathbf{g}_s , we define a decomposition $\mathbf{g}_s = \mathbf{g}_s^+ - \mathbf{g}_s^-$, where all components of vectors \mathbf{g}_s^\pm are nonnegative, and if $g_{si}^\pm \neq 0$, then $g_{si}^\mp = 0$. Let us consider the collision integral of the form:

$$\Delta = \sum_{s=1}^{n_d - n_c} \varphi_s \mathbf{g}_s \left\{ \exp(\langle \nabla H | \mathbf{g}_s^- \rangle) - \exp(\langle \nabla H | \mathbf{g}_s^+ \rangle) \right\}. \quad (6)$$

Here $\varphi_s > 0$. By construction, the collision integral (6) is admissible. If the entropy function is Boltzmann-like, and the components of the vectors \mathbf{g}_s are integers, the collision integral assumes the familiar Boltzmann-like form. An example of such a collision term for the *D2Q9*-discrete velocity model is described in Ref. [26].

2.0.3 Single relaxation time gradient model

The BGK collision integral (5) has the following important property: the linearization of the operator (5) around the local equilibrium point has a very simple spectrum $\{0, -1/\tau\}$, where 0 is the n_c -times degenerate eigenvalue corresponding to the conservation laws, while the non-zero eigenvalue corresponds to the rest of the (kinetic) eigenvectors. Nonlinear collision operators which have this property of their linearizations at equilibrium are called single relaxation time models (SRTM). They play an important role in modelling because they allow for the simplest identification of transport coefficients.

The SRTM, based on the given entropy function H , is constructed as follows (single relaxation time gradient model, SRTGM). For the system with n_c local conservation laws, let \mathbf{e}_s , $s = 1, \dots, n_d - n_c$, be an orthonormal basis in the kinetic subspace, $\langle \mathbf{m}_i | \mathbf{e}_s \rangle = 0$, and $\langle \mathbf{e}_s | \mathbf{e}_p \rangle = \delta_{sp}$. Then the single relaxation time gradient model is

$$\Delta = -\frac{1}{\tau} \sum_{s,p=1}^{n_d-n_c} \mathbf{e}_s K_{sp}(\mathbf{f}) \langle \mathbf{e}_p | \nabla H \rangle, \quad (7)$$

where K_{sp} are elements of a positive definite $(n_d - n_c) \times (n_d - n_c)$ matrix \mathbf{K} ,

$$\begin{aligned} \mathbf{K}(\mathbf{f}) &= \mathbf{C}^{-1}(\mathbf{f}), \\ C_{sp}(\mathbf{f}) &= \langle \mathbf{e}_s | \nabla \nabla H(\mathbf{f}) | \mathbf{e}_p \rangle. \end{aligned} \quad (8)$$

Here, $\nabla \nabla H(\mathbf{f})$ is the $n_d \times n_d$ matrix of second derivatives, $\partial^2 H / \partial f_i \partial f_j$. Linearization of the collision integral at equilibrium has the form,

$$\mathbf{L} = -\frac{1}{\tau} \sum_{s=1}^{n_d-n_c} \mathbf{e}_s \mathbf{e}_s, \quad (9)$$

which is obviously single relaxation time. Use of the SRTGM instead of the BGK model results in the same hydrodynamics even when the local equilibrium is not known in a closed form. Further details of this model can be found in Ref. [14].

2.0.4 H -functions of minimal kinetic models

The Boltzmann entropy function written in terms of the one-particle distribution function $f(\mathbf{x}, \mathbf{c})$ is $H = \int f \ln f d\mathbf{c}$, where \mathbf{c} is the continuous velocity. Close to the global (reference) equilibrium, this integral can be approximated by using the Gauss-Hermite quadrature with the weight

$$W = (2\pi T_0)^{(D/2)} \exp(-c^2/(2T_0)).$$

Table 1: Minimal kinetic models. Column 1: Order of Hermite velocity polynomial used to evaluate the Gauss-Hermite quadrature; Column 2: Locally conserved (hydrodynamic) fields; Column 3: Discrete velocities for $D = 1$ (zeroes of the corresponding Hermite polynomials). For $D > 1$, discrete velocities are all possible tensor products of the one-dimensional velocities in each component direction; Column 4: Weights in the entropy formula (10), corresponding to the discrete velocities of the Column 3. For $D > 1$, the weights of the discrete velocities are products of corresponding one-dimensional weights; Column 5: Macroscopic equations for the fields of Column 2 recovered in the hydrodynamic limit of the model.

1. Order	2. Fields	3. Velocities	4. Weights	5. Hydrodynamic limit
2	ρ	$\sqrt{T_0}$ $-\sqrt{T_0}$	1/2 1/2	Diffusion
3	$\rho, \rho \mathbf{u}$	0 $\sqrt{3}\sqrt{T_0}$ $-\sqrt{3}\sqrt{T_0}$	2/3 1/6 1/6	Isothermal Navier-Stokes
4	$\rho, \rho \mathbf{u}, e$	$\sqrt{3 - \sqrt{6}}\sqrt{T_0}$ $-\sqrt{3 - \sqrt{6}}\sqrt{T_0}$ $\sqrt{3 + \sqrt{6}}\sqrt{T_0}$ $-\sqrt{3 + \sqrt{6}}\sqrt{T_0}$	1/[4(3 - $\sqrt{6}$)] 1/[4(3 - $\sqrt{6}$)] 1/[4(3 + $\sqrt{6}$)] 1/[4(3 + $\sqrt{6}$)]	Thermal Navier-Stokes

Here D is the spatial dimension, T_0 is the reference temperature, while the particles mass and Boltzmann's constant k_B are set equal to one. This gives the entropy functions of the discrete-velocity models [26, 15, 16],

$$H = \sum_{i=1}^{n_d} f_i \ln \left(\frac{f_i}{w_i} \right). \quad (10)$$

Here, w_i is the weight associated with the i -th discrete velocity \mathbf{c}_i (zeroes of the Hermite polynomials). The discrete-velocity distribution functions (populations) $f_i(\mathbf{x})$ are related to the values of the continuous distribution function at the nodes of the quadrature by the formula,

$$f_i(\mathbf{x}) = w_i (2\pi T_0)^{(D/2)} \exp(c_i^2/(2T_0)) f(\mathbf{x}, \mathbf{c}_i).$$

The entropy functions (10) for various $\{w_i, \mathbf{c}_i\}$ are the only input needed for the construction of minimal kinetic models.

With the increase of the order of the Hermite polynomials used in evaluation of the quadrature (10), a better approximation to the hydrodynamics is obtained. The first few models of this sequence are represented in Table 1.

2.1 Entropic lattice Boltzmann method

If the set of discrete velocities forms the links of a Bravais lattice (with possibly several sub-lattices), then the discretization of the discrete velocity kinetic equations in time and space is particularly simple, and leads to the entropic lattice Boltzmann scheme. This happens in the important case of the isothermal hydrodynamics. The equation of the entropic lattice Boltzmann scheme reads

$$f_i(\mathbf{x} + \mathbf{c}_i \delta t, t + \delta t) - f_i(\mathbf{x}, t) = \beta \alpha(\mathbf{f}(\mathbf{x}, t)) \Delta_i(\mathbf{f}(\mathbf{x}, t)), \quad (11)$$

where δt is the discretization time step, and $\beta \in [0, 1]$ is a fixed parameter which matches the viscosity coefficient in the long-time large-scale dynamics of the kinetic scheme (11). The function α of the population vector defines the maximal over-relaxation of the scheme, and is found from the entropy condition,

$$H(\mathbf{f}(\mathbf{x}, t) + \alpha \mathbf{\Delta}(\mathbf{f}(\mathbf{x}, t))) = H(\mathbf{f}(\mathbf{x}, t)). \quad (12)$$

The nontrivial root of this equation is found for populations at each lattice site. Equation (12) ensures the discrete-time H -theorem, and is required in order to stabilize the scheme if the relaxation parameter β is close to one. We note in passing that the latter limit is of particular importance in the applications of the entropic lattice Boltzmann method to hydrodynamics because it corresponds to vanishing viscosity, and hence to numerically stable simulations of very high Reynolds number flows.

2.2 Entropic lattice BGK method (ELBGK)

An important simplification occurs in the case of the isothermal simulations when the entropy function is constructed using third-order Hermite polynomials (see Table 1): the local equilibrium population vector can be obtained in closed form [16]. This enables the simplest entropic scheme – the entropic lattice BGK model – for simulations of isothermal hydrodynamics. We present this model in dimensionless lattice units.

Let D be the spatial dimension. For $D = 1$, the three discrete velocities are

$$\mathbf{c} = \{-1, 0, 1\}. \quad (13)$$

For $D > 1$, the discrete velocities are tensor products of the discrete velocities of these one-dimensional velocities. Thus, we have the 9-velocity model for $D = 2$ and the 27-velocity model for $D = 3$. The H function is Boltzmann-like:

$$H = \sum_{i=1}^{3^D} f_i \ln \left(\frac{f_i}{w_i} \right). \quad (14)$$

The weights w_i are associated with the corresponding discrete velocity \mathbf{c}_i . For $D = 1$, the three-dimensional vector of the weights corresponding to the velocities (13) is

$$\mathbf{w} = \left\{ \frac{1}{6}, \frac{2}{3}, \frac{1}{6} \right\}. \quad (15)$$

For $D > 1$, the weights are constructed by multiplying the weights associated with each component direction.

The local equilibrium minimizes the H -function (10) subject to the fixed density and momentum,

$$\sum_{i=1}^{3^D} f_i = \rho, \quad \sum_{i=1}^{3^D} f_i c_{i\alpha} = \rho u_\alpha, \quad \alpha = 1, \dots, D. \quad (16)$$

The explicit solution to this minimization problem reads,

$$f_i^{\text{eq}} = \rho w_i \prod_{\alpha=1}^D \left(2 - \sqrt{1 + 3u_\alpha^2} \right) \left(\frac{2u_\alpha + \sqrt{1 + 3u_\alpha^2}}{1 - u_\alpha} \right)^{c_{i\alpha}}. \quad (17)$$

Note that the exponent, $c_{i\alpha}$, in (17) takes the values ± 1 , and 0 only, and the speed of sound, c_s , in this model is equal to $1/\sqrt{3}$. The factorization of the local equilibrium (17) over spatial components is quite remarkable, and resembles the familiar property of the local Maxwellians.

The entropic lattice BGK model for the local equilibrium (17) reads,

$$f_i(\mathbf{x} + \mathbf{c}_i \delta t, t + \delta t) - f_i(\mathbf{x}, t) = -\beta \alpha (f_i(\mathbf{x}, t) - f_i^{\text{eq}}(\rho(\mathbf{f}(\mathbf{x}, t)), \mathbf{u}(\mathbf{f}(\mathbf{x}, t)))). \quad (18)$$

The parameter β is related to the relaxation time τ of the BGK model (5) by the formula,

$$\beta = \frac{\delta t}{2\tau + \delta t}, \quad (19)$$

and the value of the over-relaxation parameter α is computed at each lattice site from the entropy estimate,

$$H(\mathbf{f} - \alpha(\mathbf{f} - \mathbf{f}^{\text{eq}}(\mathbf{f}))) = H(\mathbf{f}). \quad (20)$$

In the hydrodynamic limit, the model (18) reconstructs the Navier-Stokes equations with the viscosity

$$\mu = \rho c_s^2 \tau = \rho c_s^2 \delta t \left(\frac{1}{2\beta} - \frac{1}{2} \right). \quad (21)$$

The zero-viscosity limit corresponds to $\beta \rightarrow 1$.

3 Wall boundary conditions

The boundary (a solid wall) ∂R is specified at any point $\mathbf{x} \in \partial R$ by the inward unit normal \mathbf{e} , the wall temperature T_w , and the wall velocity \mathbf{u}_w . The simplest boundary condition for the minimal kinetic models is obtained upon evaluation of the diffusive wall boundary condition for the Boltzmann equation [3] with the help of the Gauss-Hermite quadrature [15, 19, 20]. The essence of the diffusive boundary condition is that particles loose their memory of the incoming direction after reaching the wall. Once a particle reaches the wall, it gets redistributed in a way consistent with the mass-balance and normal-flux conditions.

Further, the boundary condition must also satisfy the condition of detailed balance: if the incoming populations are at equilibrium (corresponding to the wall-velocity), the outgoing populations are also at equilibrium (corresponding to the wall-velocity).

For the purpose of simulations below, let us consider the case when the wall normal, \mathbf{e} , (pointing towards the fluid) is in the positive y direction. The lattice for the 9-velocity isothermal model is depicted in Fig. 1.

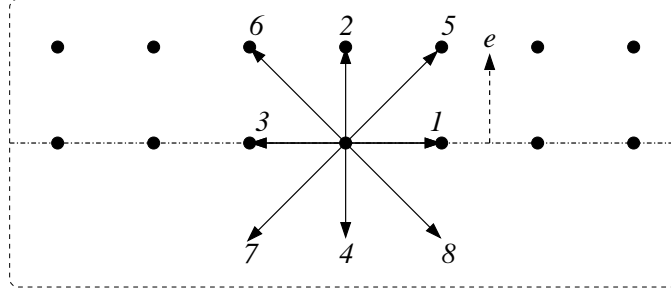


Figure 1: Schematic diagram for the situation near a flat wall, when the wall normal, \mathbf{e} , (pointing towards the fluid) is in the positive y direction.

For this particular case, the boundary update rules for incoming and grazing populations on a two-dimensional lattice are:

$$\begin{aligned}
f_0(x, y, t + \delta t) &= f_0^*(x, y, t), \\
f_1(x, y, t + \delta t) &= f_0^*(x - c\delta t, y, t), \\
f_3(x, y, t + \delta t) &= f_0^*(x + c\delta t, y, t), \\
f_4(x, y, t + \delta t) &= \frac{1}{2} [f_4^*(x, y + c\delta t, t) + f_4^*(x, y, t)], \\
f_7(x, y, t + \delta t) &= \frac{1}{2} [f_7^*(x + c\delta t, y + c\delta t, t) + f_7^*(x, y, t)], \\
f_8(x, y, t + \delta t) &= \frac{1}{2} [f_8^*(x - c\delta t, y + c\delta t, t) + f_8^*(x, y, t)],
\end{aligned} \tag{22}$$

where f^* denotes post-collision populations, and the update rules for outgoing populations are:

$$\begin{aligned}
f_2(\mathbf{x}, t + \delta t) &= f_2^{\text{eq}}(\rho, \mathbf{u}_{\text{wall}}) \frac{f_4(\mathbf{x}, t + \delta t) + f_7(\mathbf{x}, t + \delta t) + f_8(\mathbf{x}, t + \delta t)}{f_2^{\text{eq}}(\rho, \mathbf{u}_{\text{wall}}) + f_5^{\text{eq}}(\rho, \mathbf{u}_{\text{wall}}) + f_6^{\text{eq}}(\rho, \mathbf{u}_{\text{wall}})}, \\
f_5(\mathbf{x}, t + \delta t) &= f_5^{\text{eq}}(\rho, \mathbf{u}_{\text{wall}}) \frac{f_4(\mathbf{x}, t + \delta t) + f_7(\mathbf{x}, t + \delta t) + f_8(\mathbf{x}, t + \delta t)}{f_2^{\text{eq}}(\rho, \mathbf{u}_{\text{wall}}) + f_5^{\text{eq}}(\rho, \mathbf{u}_{\text{wall}}) + f_6^{\text{eq}}(\rho, \mathbf{u}_{\text{wall}})}, \\
f_6(\mathbf{x}, t + \delta t) &= f_6^{\text{eq}}(\rho, \mathbf{u}_{\text{wall}}) \frac{f_4(\mathbf{x}, t + \delta t) + f_7(\mathbf{x}, t + \delta t) + f_8(\mathbf{x}, t + \delta t)}{f_2^{\text{eq}}(\rho, \mathbf{u}_{\text{wall}}) + f_5^{\text{eq}}(\rho, \mathbf{u}_{\text{wall}}) + f_6^{\text{eq}}(\rho, \mathbf{u}_{\text{wall}})}.
\end{aligned} \tag{23}$$

4 Simulation of quasi-two-dimensional flows with two-dimensional kinetic models

As mentioned in the introduction, many microflows of engineering interest can be considered as quasi-two-dimensional. This means that averaged quantities such as flow velocity and density do not depend appreciably on the third spatial direction. Thus, it is tempting to use two-dimensional kinetic models in simulations of such flows. However, care should be taken in order to map correctly the results of two-dimensional simulations onto experimental data or molecular dynamics simulations. Indeed, molecular motion remains three-dimensional in spite of the fact that some averages can be considered two-dimensional. In the DSMC simulations of two-dimensional flows, for example, collisions of the particles are always treated as three-dimensional. The two-dimensional kinetic models therefore must be considered as a computational device which uses fictitious particles moving in two dimensions in order to mimic quasi-two-dimensional flows of particles moving in three-dimensions.

The mapping of the parameters of the three-dimensional kinetic equation onto the two-dimensional lattice Boltzmann scheme is done in two steps:

- Map the continuous 3D kinetic equation onto the 3D discrete velocity model.
- Map the 3D discrete velocity model onto the 2D velocity model.

In the case considered in this paper, the 3D continuous kinetic model is the BGK model [3], which contains the relaxation parameter τ_{BGK} ,

$$\partial_t f + c_\alpha \partial_\alpha f = -\frac{1}{\tau_{\text{BGK}}}(f - f^{\text{LM}}), \quad (24)$$

where f^{LM} is the local Maxwell distribution function. In this subsection we shall explicitly indicate all the functions and parameters related to the continuous BGK model with the subscript in order to distinguish them from the lattice counterparts.

The viscosity coefficient of the BGK model (24) is related to the relaxation time τ_{BGK} as follows:

$$\mu_{\text{BGK}} = \rho_{\text{BGK}} T_{\text{BGK}} \tau_{\text{BGK}}. \quad (25)$$

In the isothermal discrete velocity BGK model of section 2, the viscosity is expressed not as a function of temperature but of sound speed c_s ,

$$\mu = \rho c_s^2 \tau, \quad (26)$$

where $c_s = 1/\sqrt{3}$ in lattice units used in simulations. Therefore, in the first step of the above procedure, we map the parameters of the continuous 3D BGK equation onto the 3D discrete velocity model using the relation for the speed of sound, $c_{s \text{ BGK}} = \sqrt{\gamma T_{\text{BGK}}}$, where

γ is the adiabatic exponent. For an ideal gas, $\gamma = 5/3$. Thus, the first step is accomplished by the relation,

$$\begin{aligned} c_{s \text{ BGK}} &= c_s, \\ \sqrt{\frac{5}{3}T_{\text{BGK}}} &= \sqrt{\frac{1}{3}}. \end{aligned} \quad (27)$$

This formula establishes the relation between the relaxation parameter of the 3D continuous BGK equation (24) and the 3D isothermal discrete velocity model of section (2). Note that the sound speed of the thermal model is made equal to the sound speed of the isothermal model by the relation (27).

At the second step, we map the three-dimensional 27-velocity isothermal model onto the two-dimensional 9-velocity model. Note that the sound speed in both models is *identical* (and equals to $\sqrt{k_B T_0}$ in dimensional units). The mapping is done by populating at the equilibrium the links of the 27-velocity lattice in the direction orthogonal to the fixed plane containing the links of the 9-velocity sub-lattice. This amounts to the following recomputation of the three-dimensional density ρ_{3D} in terms of the two-dimensional density ρ_{2D} :

$$\rho_{3D} = \frac{3}{2}\rho_{2D}. \quad (28)$$

This formula enables the computation of the effective three-dimensional density in terms of the two-dimensional density used in the simulations with the 9-velocity model. Specification of density is an important part of the simulation since it is used to define data as prescribed pressure drop at the inlet and outlet of pipes etc.

The formulas collected in this section, together with the viscosity formula of the fully discretized entropic lattice Boltzmann method (21), enable the comparison of two-dimensional simulation results with the results obtained by microscopic simulations with different collision models (the hard sphere model, for example). The choice of the model is needed to identify the mean free path which is model-dependent, especially at moderate values of Knudsen number.

5 Plane Poiseuille flow

Plane Poiseuille flow is one of the most studied benchmarks on gas dynamics. The gas moves between two parallel plates driven by a fixed pressure difference between the inlet and outlet. It is well known that for this setup the flow rate through a cross-section of the pipe exhibits a minimum [27, 3]. In fact, one of the major achievements in the early days of kinetic theory was the prediction of a minimum of the mass flow rate as a function of the Knudsen number for $Kn \sim 1$.

We simulate the two-dimensional flow in a rectangular duct of length L along the streamwise direction (x) and width $H \ll L$ along the wall-normal (y) direction. The flow is driven by a fixed pressure difference $\Delta P = P_{\text{in}} - P_{\text{out}}$, where P_{in} and P_{out} are the pressure at the inlet and outlet of the duct, respectively. In the subsequent analysis, we shall follow

the convention used by Cercignani, where the Knudsen number for the BGK model is defined as (continuous BGK units):

$$\text{Kn} = \frac{\mu\sqrt{2T_0}}{P_0H}, \quad (29)$$

where the pressure P_0 is defined as the mean of the inlet and outlet pressures, $P_0 = (P_{\text{in}} + P_{\text{out}})/2$. In the hydrodynamic limit, this results in the well known Hagen-Poiseuille parabolic velocity profile:

$$u(y) = U_0 \left(\frac{1}{4} - \frac{y^2}{H} \right), \quad (30)$$

where the amplitude of the flow for a two-dimensional duct is $U_0 = H^2\Delta P/(2\mu L)$. From the analysis of the Boltzmann-BGK equation it is known that the dimensionless flow rate

$$Q = \frac{1}{HU_0\text{Kn}} \int_{H/2}^{H/2} u(y)dy, \quad (31)$$

has a low-Knudsen ($\text{Kn} \ll 1$) asymptotic:

$$Q_0 = \frac{1}{6\text{Kn}} + s + (2s^2 - 1) \text{Kn}, \quad (32)$$

with $s = 1.015$ (see [3]), which is equivalent to solving the Navier-Stokes equation with a second-order slip boundary condition. Further, the high-Knudsen asymptotic expression for the flow rate is:

$$Q_\infty \sim \frac{1}{\sqrt{\pi}} \log(\text{Kn}) + O(1), \quad (33)$$

which implies a slow logarithmic divergence of the flow rate as a function of the Knudsen number. These two asymptotic limits ensure that the flow rate must have at least one minimum at some finite Kn. The low-Knudsen asymptotic behavior is related to the situation where on the average the number of collisions encountered by a molecule in the bulk is much larger than the collisions with the wall. Thus, the effective balance between the frictional forces (due to collisions) and the applied pressure gradient ensures a parabolic velocity profile (with a slip at the wall). On the other hand, any molecular motion in high Knudsen number flows is retarded mostly by collisions occurring at the wall. This leads to an effectively flat velocity profile in the channel.

In addition to the asymptotic analysis, more detailed investigations of the linearized Boltzmann equation are available (see, for example, [28]). In the next subsection, we compare the result of our numerical simulation with the numerical result of [28] and the asymptotic expressions.

5.1 Numerical simulation

Poiseuille flow in a two-dimensional duct was simulated with the entropic LBGK model for a range of Knudsen numbers. The length to height ratio used in the simulation was 30, and the resolution was taken 1101×45 points. In lattice units, the Knudsen number is:

$$\text{Kn} = \frac{\tau}{H} \sqrt{\frac{2}{5}}. \quad (34)$$

The simulation results for the flow-rate is plotted in Fig. 2 together with the numerical solution of the stationary linearized BGK model [28] and the asymptotic expressions. Some of the important conclusions following from this study are:

- Quantitative agreement with the fully microscopic results is obtained in the range of $0 \leq \text{Kn} \leq 0.01$. This indicates that the *parameter-free* ELBGK model can be used in the domain of slip-flow for quantitative simulations.
- At higher Knudsen numbers, the simulation results predict the expected logarithmic divergence (as indicated by the dashed line in Fig. refFig:Flowrate), but they do deviate from the numerical solution of the linearized stationary BGK equation. At very high Knudsen numbers, the finite size of the duct will always lead to a nearly flat (independent of Kn) flow rate.
- Our simulations predict the Knudsen minimum at moderate values of Kn. The minimum is found around $\text{Kn} = 0.35$, whereas much more elaborate (and computationally expensive) molecular dynamics simulations [2] and the semi-analytical solutions to the stationary BGK equation indicate the location of the minimum at Kn in the range $0.8 - 1$. The discrepancy is not surprising because the model used in our simulation is drastically simpler than any of the alternative models. In particular, the built-in isothermal assumption limits its domain of validity to the cases when incompressibility is a good approximation indeed (slip-flow). In the domain of $\text{Kn} \sim 1$ it is therefore required to use the non-isothermal model which includes correctly the energy redistribution in the collision processes.

6 Discussion and conclusions

In this paper, we have set up the basis of a new computational approach for the simulation of microflows - the entropic lattice Boltzmann method. We have described the hierarchy of entropic lattice Boltzmann models for both isothermal and thermal simulations. Here, we have focused on the simplest isothermal model - the entropic lattice BGK equation and presented in detail the implementation of the diffusive wall boundary condition in the lattice Boltzmann setting. For the ELBGK model, we derived the parameter map of two-dimensional isothermal simulations on the three-dimensional data, and have tested all this on the benchmark problem of the planar Poiseuille flow in the full range of rarefaction

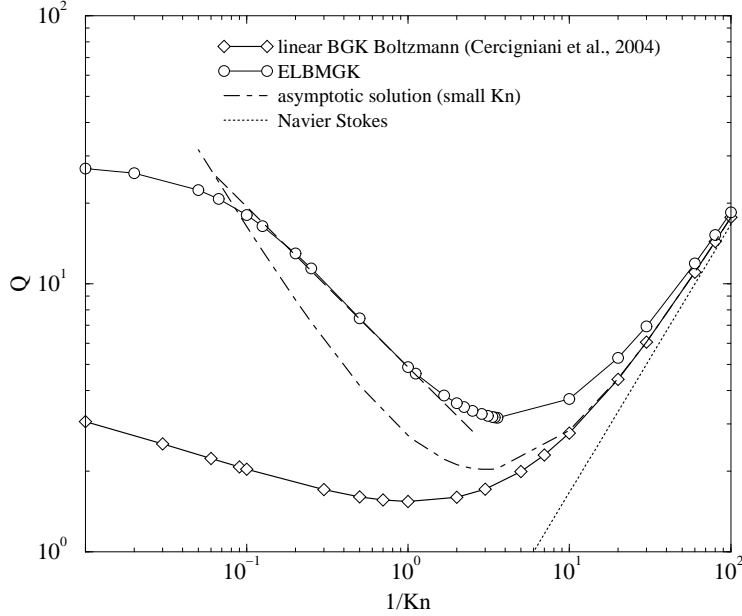


Figure 2: Comparison of the ELBM solution for the dimensionless flow rate with the low Kn asymptotic solution, and the numerical solution of the stationary linearized BGK equation [28]. The dashed line indicates the qualitative agreement with the expected logarithmic scaling at higher Kn. All the curves become indistinguishable at $\text{Kn} \leq 0.01$.

(Knudsen number) from the nearly-continuous case to the free-molecular flow. Thus, we confirm the validity of the entropic lattice Boltzmann method as a viable tool for computations of the microflows in the most relevant to MEMS applications domain of Kn up to $\text{Kn} \sim 0.1$. This confirmation clearly points to the usefulness of development of more sophisticated lattice Boltzmann models in this range of parameters which is the subject of further studies. It should be stressed that applications of the isothermal models can be considered as a parameter-free slip-flow hydrodynamic models, and that the way to extend the domain of the quantitative predictions must take into account energy conservation in the collisions. We would also like to point out the computational efficiency of the proposed models. For example, the full data set presented in Fig. 2 was computed within several hours on a single-processor computer facility.

Finally, let us briefly mention the following by-product of our study, relevant for the use of the lattice Boltzmann simulations in molecular models. In particular, the Direct Simulation Monte Carlo method (DSMC) requires a good initial choice of the velocity distribution function to perform efficiently. Most of the current simulations use the local equilibrium (or equilibrium) Maxwell distribution function. A better choice could be the anisotropic Gaussian approximation

$$f(\mathbf{v}, \mathbf{x}) \sim \exp \left(-(v_\alpha - u_\alpha) \rho P_{\alpha\beta}^{-1} (v_\beta - u_\beta) \right), \quad (35)$$

where P^{-1} is the inverse of the pressure tensor,

$$P_{\alpha\beta} = \int \frac{(v_\alpha - u_\alpha)(v_\beta - u_\beta)}{2} f d\mathbf{v}. \quad (36)$$

The LB data for the stationary stress tensor and for the flow field can be used as initial guess for the functions $u_\alpha(\mathbf{x})$ and $P_{\alpha\beta}^{-1}(\mathbf{x})$ in the velocity distribution function (35). This initial condition for the DSMC simulation of the stationary will dramatically reduce the simulation time as compared to the case when it is initialized at equilibrium.

Acknowledgments. This work was supported by the Bundesamt für Energie, BFE-Project Nr. 100862 "Lattice Boltzmann simulations for chemically reactive systems in a micrometer domain". Discussions with A. N. Gorban, S. Succi, A. Tomboulides and F. Toschi are kindly acknowledged.

References

- [1] C.-M. Ho and Y.-C. Tai. Micro-electro-mechanical-systems(MEMS) and fluid flows. *Annu. Rev. Fluid Mech.*, 30:579–612, 1998.
- [2] A. Beskok and G. E. Karniadakis. *Microflows: Fundamentals and Simulation*. Springer, Berlin, 2001.
- [3] C. Cercignani. *Theory and Application of the Boltzmann Equation*. Scottish Academic Press, Edinburgh, 1975.
- [4] Y. Sone. *Kinetic Theory and Fluid Dynamics*. Birkhäuser, Basel, 2002.
- [5] G. A. Bird. *Molecular Gas Dynamics and the Direct Simulation of Gas Flows. Theory and Application of the Boltzmann Equation*. Clarendon Press, Oxford, 1994.
- [6] E. S. Oran, C. K. Oh, and B. Z. Cybyk. Direct simulation Monte Carlo: Recent advances and applications. *Annu Rev. Fluid Mech.*, 30:403–441, 1998.
- [7] A. N. Gorban and I. V. Karlin. *Invariant Manifolds for Physical and Chemical Kinetics. Lec. Notes Phys. 660*. Springer, Berlin, 2004.
- [8] H. Grad. On the kinetic theory of rarefied gases. *Comm. Pure Appl. Math.*, 2:331, 1949.
- [9] M Grmela, I. V. Karlin, and V. B. Zmievski. Boundary layer variational principle: A case study. *Phys. Rev. E*, 66:011201(1–12), 2002.
- [10] I. V. Karlin, A. Gorban, S. Succi, and V. Boffi. Maximum entropy principle for lattice kinetic equations. *Phys. Rev. Lett.*, 81:6–9, 1998.
- [11] A. J. Wagner. An H -Theorem for the Lattice Boltzmann Approach to Hydrodynamics. *Europhys. Lett.*, 44:144–149, 1998.

- [12] S Ansumali and I. V. Karlin. Stabilization of the Lattice Boltzmann Method by the H Theorem: A Numerical Test. *Phys. Rev. E*, 62:7999–8003, 2000.
- [13] S Ansumali and I. V. Karlin. Entropy function approach to the lattice Boltzmann method. *J. Stat. Phys.*, 107:291–308, 2002.
- [14] S Ansumali and I. V. Karlin. Single relaxation time model for entropic lattice Boltzmann methods. *Phys. Rev. E*, 65:056312, 2002.
- [15] S. Ansumali and I. V. Karlin. Kinetic Boundary Condition for the Lattice Boltzmann Method. *Phys. Rev. E*, 66:026311, 2002.
- [16] S. Ansumali, I. V. Karlin, and H. C. Öttinger. Minimal entropic kinetic models for simulating hydrodynamics. *Europhys. Lett.*, 63:798–804, 2003.
- [17] B. M. Boghosian, J Yepez, P. V. Coveney, and A. J. Wagner. Entropic lattice Boltzmann methods. *Proc. Roy. Soc. Lond. A*, 457:717–766, 2001.
- [18] S Succi, I. V. Karlin, and H. Chen. Role of the h theorem in lattice Boltzmann hydrodynamics. *Rev. Mod. Phys.*, 74:1203, 2002.
- [19] S. Ansumali, S. S. Chikatamarla, C. M. Frouzakis, and K. Boulouchos. Entropic lattice Boltzmann simulation of the flow past square cylinder. *Int. J. Mod. Phys. C*, 15(3):435–445, 2004.
- [20] X. D. Niu, C. Shu, and Y.T. Chew. Lattice boltzmann BGK model for simulation of micro flows. *Euro. Phys. Lett.*, 67:600–606, 2004.
- [21] S. Succi. *The Lattice Boltzmann Equation for Fluid Dynamics and Beyond*. Oxford University Press, Oxford, 2001.
- [22] X. Nie, G. Doolen, and S. Chen. Lattice-Boltzmann simulations of fluid flows in MEMS. *J. Stat. Phys.*, 107:279–289, 2002.
- [23] C. Y. Lim, C. Shu, X. D. Niu, and Y. T. Chew. Application of lattice boltzmann method to simulate microchannel flows. *Phys. Fluid*, 107:2299–2308, 2002.
- [24] S. Succi. Mesoscopic modeling of slip motion at fluid-solid interfaces with heterogeneous catalysis. *Phys. Rev. Lett.*, 89:064502, 2002.
- [25] B. Li and D. Kwok. Discrete boltzmann equation for microfluidics. *Phys. Rev. Lett.*, 90:124502, 2003.
- [26] I. V. Karlin, A Ferrante, and H. C. Öttinger. Perfect entropy functions of the lattice Boltzmann method. *Europhys. Lett.*, 47:182–188, 1999.
- [27] M Knudsen. Die gesetze der molekulären Strömung und der inneren Reibungsströmung der Gase durch Röhren. *Ann. der Physik*, 28:75–130, 1909.

- [28] C. Cercignani, M. Lampis, and S. Lorenzani. Variational approach to gas flows in microchannels. *Phys. Fluid*, 16:3426–3437, 2004.